Brain Research 1733 (2020) 146720

Contents lists available at ScienceDirect

Brain Research

journal homepage: www.elsevier.com/locate/brainres

Research report

Effects of mTOR inhibitors on neuropathic pain revealed by optical imaging of the insular cortex in rats

Kyeongmin Kim[a,b,1], Songyeon Choi[a,b,1], Myeounghoon Cha[a], Bae Hwan Lee[a,b,*]

[a] Department of Physiology, Yonsei University College of Medicine, Seoul 03722, Republic of Korea
[b] Brain Korea 21 PLUS Project for Medical Science, Yonsei University College of Medicine, Seoul 03722, Republic of Korea

HIGHLIGHTS

- Mechanical allodynia was alleviated after treatment with ATP-competitive mTOR inhibitors.
- The optical signals in the IC decreased after Torin1 and XL388 treatments.
- mTOR complex could be modulated for a more effective treatment of intractable pain.

ARTICLE INFO

Keywords:
Neuropathic pain
insular cortex (IC)
Optical imaging
mTOR complex
Cortical activity

ABSTRACT

In the pain matrix, the insular cortex (IC) is mainly involved in discriminative sensory and motivative emotion. Abnormal signal transmission from injury site causes neuropathic pain, which generates enhanced synaptic plasticity. The mammalian target of rapamycin (mTOR) complex is the key regulator of protein synthesis; it is involved in the modulation of synaptic plasticity. To date, there has been no report on the changes in optical signals in the IC under neuropathic condition after treatment with mTOR inhibitors, such as Torin1 and XL388. Therefore, we aimed to determine the pain-relieving effect of mTOR inhibitors (Torin1 and XL388) and observe the changes in optical signals in the IC after treatment. Mechanical threshold was measured in adult male Sprague-Dawley rats after neuropathic surgery, and therapeutic effect of inhibitors was assessed on post-operative day 7 following the microinjection of Torin1 or XL388 into the IC. Optical signals were acquired to observe the neuronal activity of the IC in response to peripheral stimulation before and after treatment with mTOR inhibitors. Consequently, the inhibitors showed the most effective alleviation 4 h after microinjection into the IC. In optical imaging, peak amplitudes of optical signals and areas of activated regions were reduced after treatment with Torin1 and XL388. However, there were no significant optical signal changes in the IC before and after vehicle application. These findings suggested that Torin1 and XL388 are associated with the alleviation of neuronal activity that is excessively manifested in the IC, and is assumed to diminish synaptic plasticity.

1. Introduction

Pain is considered as a signal from our body that helps detect noxious stimuli or lesions. Acute pain can often be converted into chronic pain due to various reasons, such as nerve or tissue injury, inflammation, tumor growth, and viral infection (Kuner and Flor, 2016). These factors can also lead to neuropathic pain that induces hyperalgesia, allodynia, and spontaneous pain, which are identified by

Abbreviations: ACC, anterior cingulate cortex; AI, agranular insular cortex; AID, agranular insular cortex, dorsal part; AIV, agranular insular cortex, ventral part; AP, anterior to posterior; ATP, adenosine triphosphate; DI, dysgranular insular cortex; eIF4E, eukaryotic translation initiation factor 4E; FKBP12, FK-binding protein 12; GI, granular insular cortex; IC, insular cortex; LTP, long-term potentiation; NP, nerve-injured; PODs, post-operative days; 4EBPs, 4E-binding proteins; p70S6K, ribosomal protein p70 S6 kinase; ERK, extracellular signaling-regulated kinases; MCA, middle cerebral artery; mTOR, mammalian target of rapamycin; mTORC1, mammalian target of rapamycin complex 1; mTORC2, mammalian target of rapamycin complex 2; ROI, region of interest; RV, rhinal vein; S1, primary somatosensory cortex; S2, secondary somatosensory cortex; Sham, sham-injured; VSD, voltage-sensitive dye; FRB, FKBP-rapamycin binding protein; two-way ANOVA, two-way repeated-measures analysis of variance; PKC α, protein kinase C α; PIKK, phosphatidyl inositol 3′ kinase-related kinases; PDK1, Phosphoinositide-dependent kinase-1; AKT, protein kinase B; RAIC, rostral anterior insular cortex; SEM, standard error of the mean

* Corresponding author at: Department of Physiology, Yonsei University College of Medicine, 50-1, Yonsei-ro, Seodaemun-gu, Seoul 03722, Korea.
E-mail address: bhlee@yuhs.ac (B.H. Lee).
[1] These authors contributed equally to this work.

https://doi.org/10.1016/j.brainres.2020.146720
Received 29 August 2019; Received in revised form 22 January 2020; Accepted 7 February 2020
Available online 14 February 2020

abnormal sensory perception and stimulus-independent persistent pain (Callin and Bennett, 2008; Jaggi and Singh, 2011). Although many drugs are being developed to treat chronic pain, approximately 4–8% of patients worldwide are still suffering from chronic pain as well as unexpected side effects of the drugs (Li et al., 2016; Xu et al., 2012).

Recently, many studies have attempted to modulate the activation of various regions of the brain for attenuating neuropathic pain (Cha et al., 2017; Li et al., 2010; Metz et al., 2009). Regions of the brain that participate in pain perception are involved in sensory-discriminative properties or emotional aspects of pain (Apkarian et al., 2005; Basbaum et al., 2009). Such regions of the brain—that is, the anterior cingulate cortex (ACC), insular cortex (IC), primary somatosensory cortex (S1), secondary somatosensory cortex (S2), and prefrontal cortex—constitute the "pain matrix" (Garcia-Larrea and Peyron, 2013).

Among the regions constituting the pain matrix, the IC is mainly associated with sensory discernment and emotion of pain (Lu et al., 2016). Anterior part of the IC is cytoarchitectonically interconnected with the limbic cortex, which regulates somatic nociceptive and visceral inputs (Jasmin et al., 2004; Lutz et al., 2013). This morphological evidence indicates that rostral part of the IC is identified in sensory discernment and emotional processing of nociception (Lu et al., 2016). Furthermore, when a lesion occurs in the rostral anterior IC, pain-like behavior is significantly diminished (Coffeen et al., 2011). Human brain imaging studies showed an increased neuronal activity in the IC after high-intensity noxious stimulation (Baumgärtner et al., 2010; Craig et al., 2000; Hess et al., 2007; Lorenz and Casey, 2005; Lorenz et al., 2002).

The abnormal signals resulting from neuropathic pain alter synapses and neurotransmitter properties, leading to long-term potentiation (LTP) (Kuner, 2010; Kuner and Flor, 2016; Luo et al., 2014; Zhuo, 2008). LTP is affected by specific RNA-binding proteins and signal transduction cascades, which modulate the initiation of mRNA translation (Klann et al., 2004; Pfeiffer and Huber, 2006). Major key regulators of mRNA translation are known as multiple extracellular signaling-regulated kinases (ERK) and mammalian target of rapamycin (mTOR) signaling pathways.

mTOR complex is a serine/threonine kinase, and it also affects cell growth, cell proliferation, cell survival, and hormone regulation. Rapamycin and rapalogs, which have been called the first-generation mTOR inhibitors (Vilar et al., 2011), were developed for treating neuropathic pain (Liu et al., 2009; Martelli et al., 2018); however, these drugs were shown to be associated with side effects and limitations related to alleviation of neuropathic pain (Guertin and Sabatini, 2009). These limitations were expected due to the incomplete inhibition of mTOR complex and the existence of feedback loop (Guertin and Sabatini, 2009; Vilar et al., 2011). For complete inhibition of mTOR complex, the second-generation mTOR inhibitors, called adenosine triphosphate (ATP)-competitive inhibitors, were developed (Albert et al., 2010). However, there is no electrophysiology- or optical imaging-based evidence on the alleviation of neuropathic pain induced by Torin1 and XL388.

To observe the changes in cortical excitability in the state of pain, many researchers have performed optical imaging, as it could directly measure the membrane potential changes and allow high-resolution imaging of superficial brain structures (Cha et al., 2009; Chae et al., 2010; Ferezou et al., 2009; Han et al., 2016; Kim et al., 2018). This method helps reflect the membrane responses following changes in neurons using a voltage-sensitive dye (VSD), which is sensitive to rapid and linear membrane potential changes (Fehervari et al., 2015; Ferezou et al., 2009; Fujita et al., 2010; Kobayashi et al., 2010).

Therefore, the purpose of the current study was to investigate the correlation between the alleviative effect of mTOR inhibition on neuropathic pain and the changes in pain-related neuronal activity patterns in the IC. In this study, we elucidated the alleviative effect of ATP-competitive mTOR inhibitors Torin1 and XL388 by comparing the spatiotemporal patterns of cortical excitability using VSD imaging of the IC in neuropathic rats.

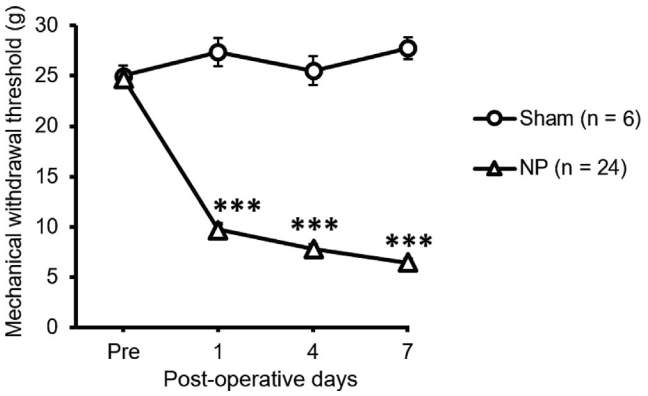

Fig. 1. Development of mechanical allodynia in sham-injured (Sham) and nerve-injured (NP) rats. As neuropathic pain progressed, mechanical withdrawal threshold changed significantly on post-operative days (PODs) 1, 4, and 7. Data are presented as means ± standard error of the mean (SEM). ***$p < 0.001$ vs. sham, as determined by two-way repeated-measures analysis of variance (two-way ANOVA) followed by Bonferroni's post-hoc multiple comparison test.

2. Results

2.1. Development of mechanical allodynia induced by peripheral nerve injury

We measured withdrawal threshold on the injured hind paw using the electronic von Frey filament on PODs 1, 4, and 7 (Fig. 1). The mechanical withdrawal threshold of nerve-injured group decreased significantly from POD 1 to POD 7, and these values were significantly lower than the corresponding values of sham-injured group ($p < 0.001$, two-way ANOVA followed by Bonferroni's post-hoc multiple comparison test). However, the mechanical withdrawal threshold had not shown any difference between groups before surgery ($p > 0.05$).

2.2. Microinjection of Torin1 and XL388 into the IC reduces mechanical allodynia

To investigate the effect of mTOR inhibition on neuropathic pain, vehicle, Torin1, or XL388 were administered directly into the IC on POD 7 by microinjection. Fig. 2A shows the locations of the injection cannula tips in each group. The changes in mechanical withdrawal threshold were examined 30 min and 1, 2, 4, 8, 12, and 24 h after microinjection (Fig. 2B). The pain-relieving effect significantly increased from 1 h to 4 h after Torin1 microinjection in NP group ($p < 0.05$, $n = 8$, two-way ANOVA followed by Bonferroni's post-hoc multiple comparison test). Meanwhile, considerable pain alleviation was observed only for 4 h after XL388 microinjection in NP group ($p < 0.01$, $n = 8$). Both drugs significantly inhibited mechanical allodynia 4 h after injection of each drug. The pain alleviative effect of both drugs decreased 8 h after microinjection, and it reached the threshold of the vehicle 24 h after microinjection. There were no significant changes after vehicle microinjection in sham group during 24-h period after microinjection ($p > 0.05$, $n = 6$). In vehicle-treated NP group showed no changes in threshold during the 24-h period after microinjection ($p > 0.05$, $n = 8$).

2.3. Correlation between electrical stimulation and optical responses in the IC

To confirm the correlation of optical responses in the IC and

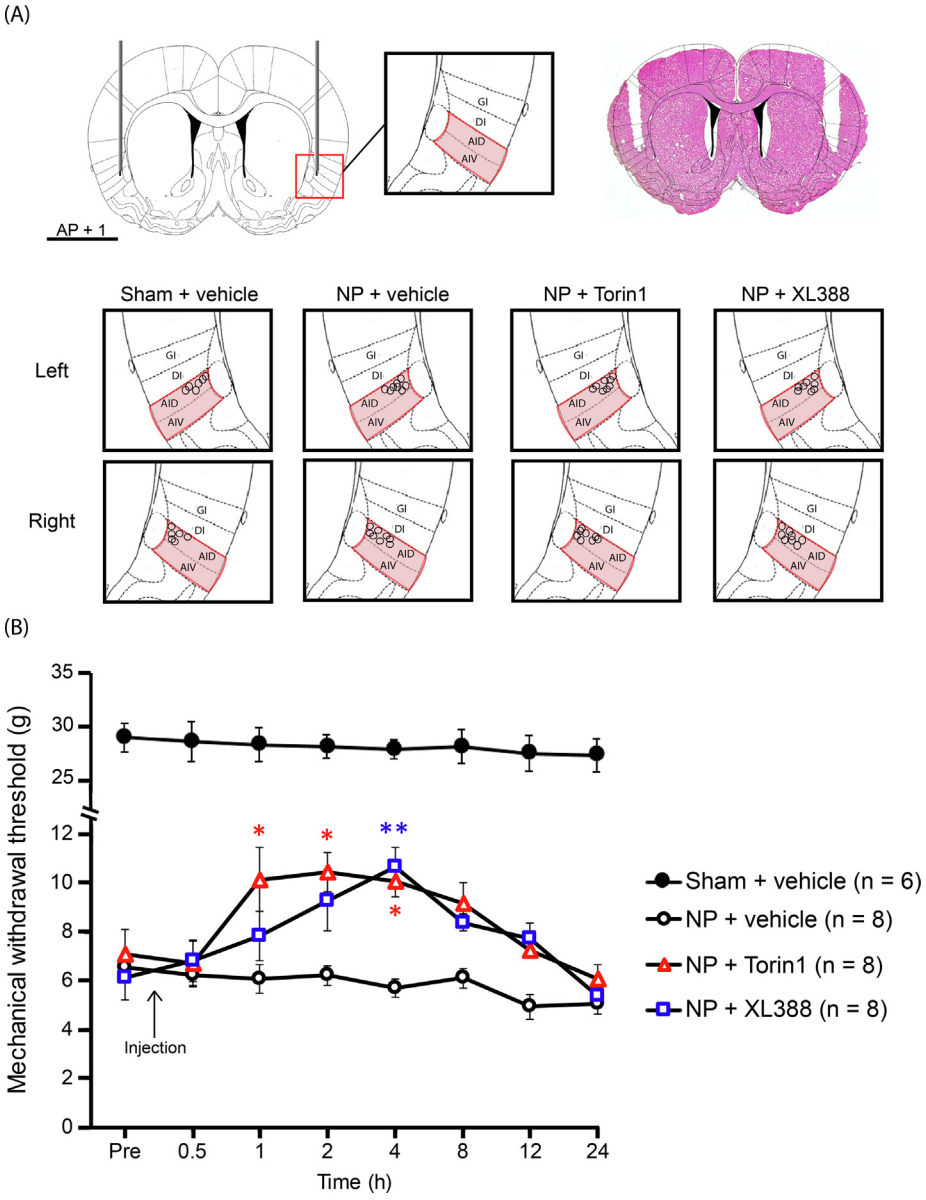

Fig. 2. Illustration of stereotaxic implantation of guide cannulae and the changes of mechanical threshold following microinjection of vehicle, Torin1, or XL388. (A) Histological identification of the rostral anterior insular cortex (RAIC) with rat atlas (Paxinos and Watson, 2006) using hematoxylin-eosin stain. The RAIC was located 1 mm anteriorly from the bregma (AP + 1). Subdivisions of the IC are included in the black square box. Small circles in the black square box indicate the locations of the injection cannulae in each group. (B) The pain-relieving effect following microinjection of vehicle, Torin1, or XL388 into the IC on POD 7. Data are presented as means ± SEM. *p < 0.05, **p < 0.01 vs. vehicle, as determined by two-way ANOVA followed by Bonferroni's post-hoc multiple comparison test.

electrical stimulation of peripheral receptive field, Pearson's correlation coefficient was calculated. Since the correlation coefficient was higher than 0.7, high correlation was confirmed between the peak amplitudes of optical signals and intensity of electrical stimulation in vehicle-treated NP group ($p < 0.001$, $r = 0.8088$, $n = 8$, one sample *t*-test, Fig. 3A), Torin1-treated NP group ($p < 0.001$, $r = 0.8478$, $n = 8$, Fig. 3C), and XL388-treated NP group ($p < 0.001$, $r = 0.7816$, $n = 8$, Fig. 3E) before treatment. Before the application of mTOR inhibitors, the high value of correlation coefficient indicated that there is a high correlation between peak amplitudes and intensity of electrical stimulation in all of the groups. After treatment with the vehicle in NP groups, correlation coefficient remained high ($p < 0.001$, $r = 0.7868$, $n = 8$, Fig. 3A). However, correlation coefficients were lower after treatment with Torin1 ($p > 0.05$, $r = 0.2710$, $n = 8$, Fig. 3C) or XL388 ($p > 0.05$, $r = 0.1582$, $n = 8$, Fig. 3E) in NP groups. In Fig. 3B, D, and F, the region outlined with red indicates the activated area of the IC before the application of vehicle or mTOR inhibitors, and the region outlined with blue shows the activated areas after treatment with vehicle or mTOR inhibitors. When electrical stimulation of the highest intensity was applied to the nerve-injured hind paw, activation was generally observed at granular insular cortex (GI), dysgranular insular cortex (DI) in all groups before application of vehicle or mTOR inhibitors (Fig. 3B, D, and F). After treatment with Torin1 and XL388, the activation area of optical signals was noticeably decreased; however, after treatment with the vehicle, broad activated areas still remained.

2.4. Changes in optical signals in the IC induced by Torin1 and XL388

Optical imaging using VSD demonstrates intuitive observation of cortical activation. In this study, we observed the changes in cortical activity of the IC in response to the electrical stimulation (0, 0.6, 1.25, 2.5, and 5 mA) applied to the nerve-injured paw of sham-surgery or neuropathic rats. Fig. 4 compares the peak amplitudes of optical signals in response to electrical stimulation before and after treatment with the vehicle in sham group, vehicle, Torin1, or XL388 in NP group (Fig. 4A, B, I, and J). The peak amplitude of cortical activity in the IC was confirmed by maximal intensity value of optical signals (Fig. 4C, D, K, and L). Each orange and blue line indicates averaged and filtered optical intensity of the IC of the rats before and after application of vehicle or mTOR inhibitors, respectively. Significant differences were not observed between peak amplitudes before and after vehicle treatment in sham group ($p > 0.05$, $n = 5$, two-way ANOVA, Fig. 4E). There were

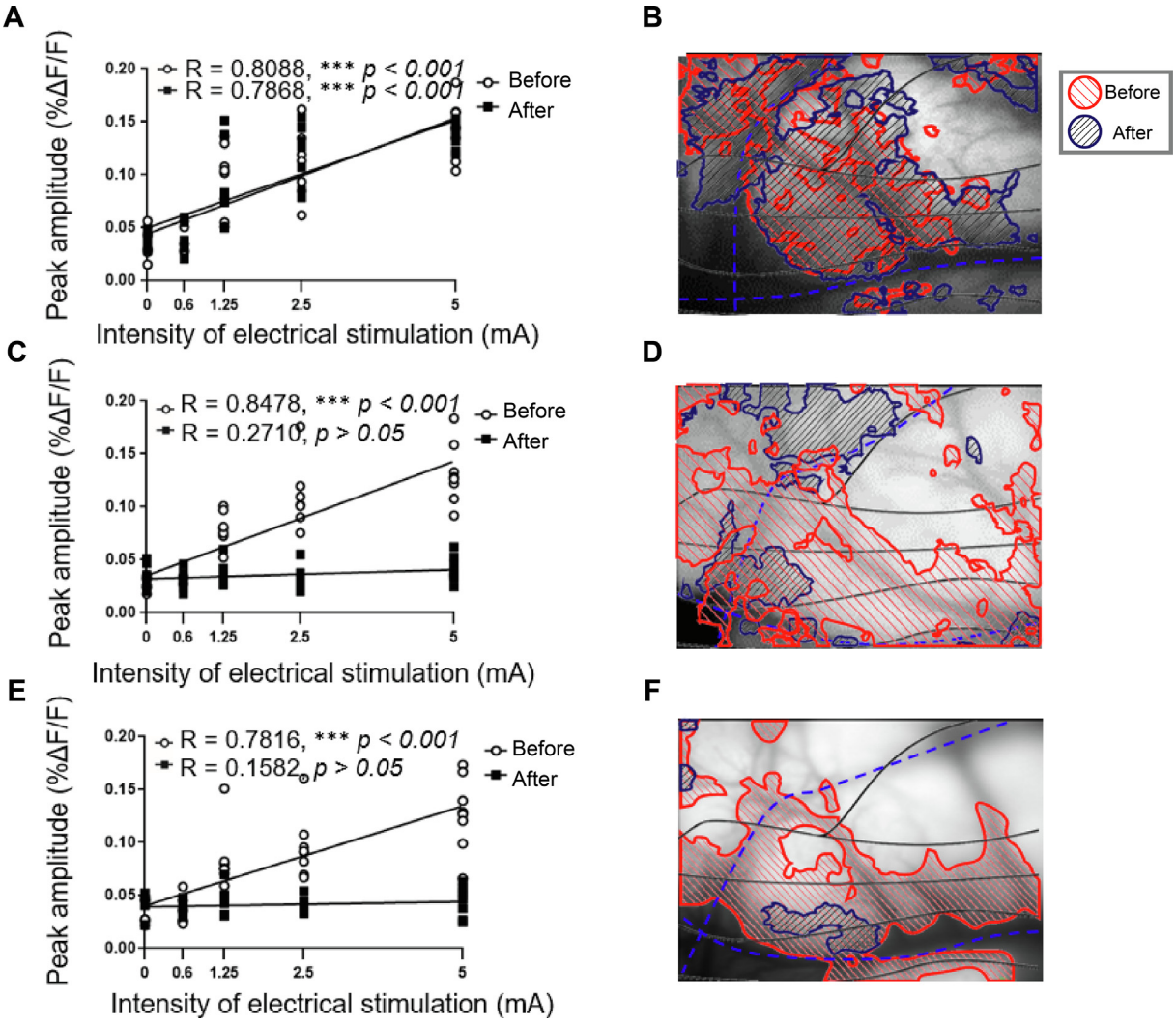

Fig. 3. Correlation of optical signals in the IC and intensity of electrical stimulation on the peripheral receptive field of the injured hind paw before and after treatment with the vehicle, Torin1, or XL388 in NP groups. The peak amplitudes of optical signals before and after treatment with the vehicle (A), Torin1 (C), or XL388 (E) are plotted against the intensity of electrical stimulation. Pearson's correlation coefficients (R) and p values are provided on the top left side of each graph. Intuitive images of the area activated by electrical stimulation through optical imaging before and after treatment with the vehicle (B), Torin1 (D), or XL388 (F). ***$p < 0.001$ indicates that the correlation coefficient is statistically significant.

no significant differences between peak amplitudes before and after vehicle treatment in neuropathic rats ($p > 0.05$, $n = 8$, two-way ANOVA, Fig. 4F). In Torin1- and XL388-treated NP groups, the peak amplitude of cortical activity increased proportionally with an increase in the intensity of electrical stimulation before treatment. On the contrary, the peak amplitude of cortical activity was significantly reduced after treatment with Torin1 and XL388 ($p < 0.001$, two-way ANOVA, Fig. 4M and N). The peak amplitudes of optical activity at electrical stimulation intensities of 1.25, 2.5, and 5 mA after the application of Torin1 were significantly lower than those before treatment ($p < 0.001$, $n = 8$, two-way ANOVA, Fig. 4M). The peak amplitudes of optical signals in the IC at electrical stimulation intensities of 1.25, 2.5, and 5 mA were significantly lower after treatment with XL388 than they were before treatment ($p < 0.001$, $n = 8$, two-way ANOVA, Fig. 4N). To compare the activated areas of the IC in response to electrical stimulation, a circle with a radius of 20 pixels was set. Prior to the application of vehicle, Torin1, or XL388 onto the IC in all groups, the area of activated region increased with an increase in the intensity of electrical stimulation of the hind paw (Fig. 4G, H, O, and P). After the application of vehicle in sham and NP group, no significant changes in the areas of activated regions of the IC were observed ($p > 0.05$, two-way ANOVA, Fig. 4G and H). However, the area of activated region of the IC reduced significantly after Torin1 or XL388 treatment ($p < 0.05$, two-way ANOVA, Fig. 4O and P). The peak amplitudes of optical signals were restored 2 h after Torin1 or XL388 was washed (Supplementary Fig. 1). Besides, the peak amplitudes of optical signals and areas of activated regions in sham group were not shown significant changes after the application of vehicle, Torin1 or XL388 (Supplementary Fig. 2). This was to confirm whether the alleviation effect of Torin1 or XL388 was caused by neuronal toxicity. These results indicated that Torin1 and XL388 do not induce neuronal toxicity.

2.5. Stripe analysis of optical signals in the IC induced by electrical stimulation

To analyze the spatial and temporal patterns of optical signals in the IC, a stripe analysis of optical activity was performed (Fig. 5). Analysis of stripe images was suitable for observing temporal variations of optical activity within a particular region in different directions. In Fig. 5, spatiotemporal patterns of neural activity were obtained from the line in the corresponding optical images on the left side. In temporal analysis, vehicle-treated NP group showed prolonged excitation signals

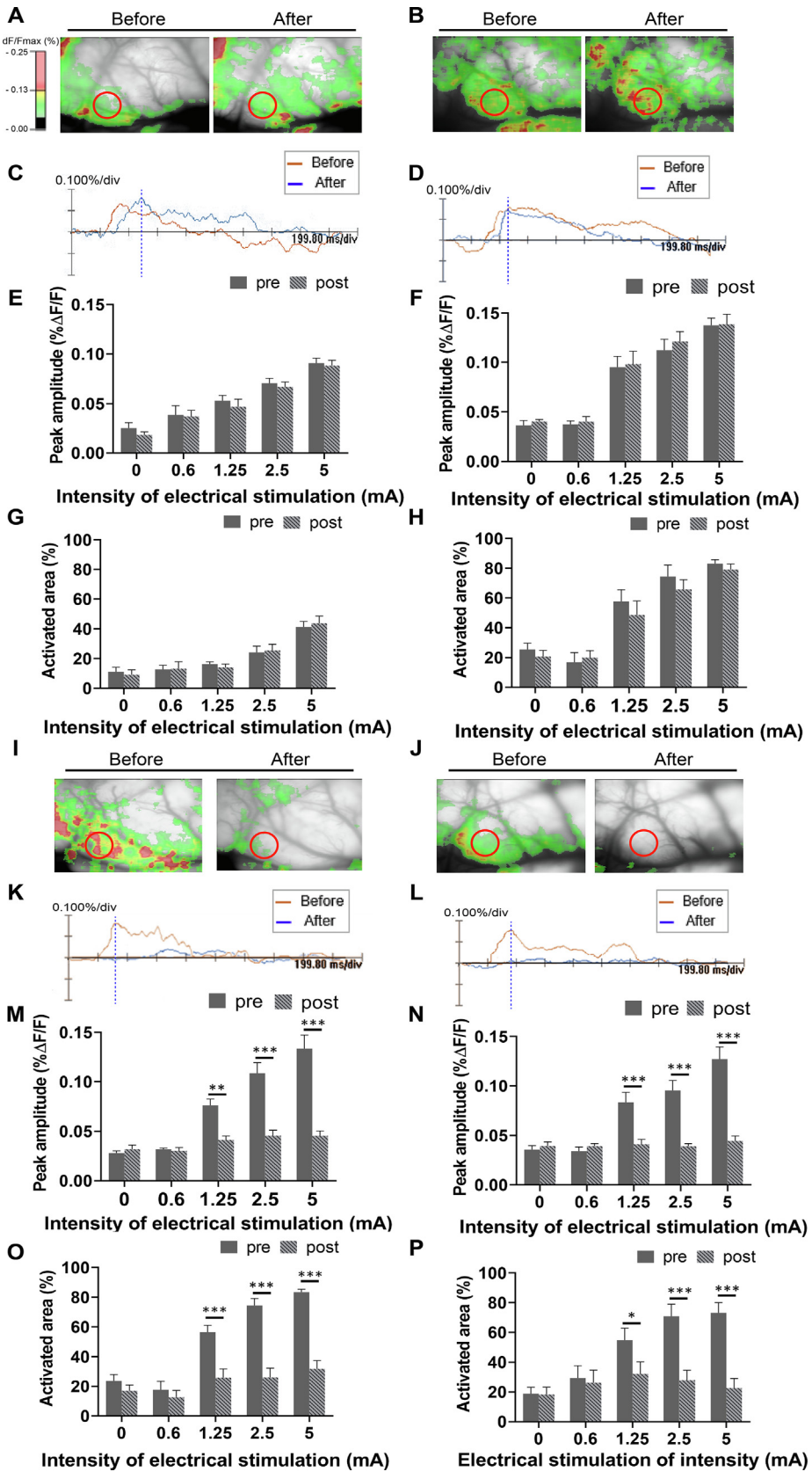

Fig. 4. Comparison of peak amplitudes and activated areas before and after treatment with the vehicle, Torin1, or XL388. Representative optical images of the IC before and after treatment with the vehicle in sham group (A), and vehicle (B), Torin1 (I), XL388 (J) in NP group. Representative optical signals from the IC before and after treatment with the vehicle in sham group (C), and vehicle (D), Torin1 (K), XL388 (L) in NP group. Comparison of peak amplitudes before and after treatment with the vehicle in sham group (E), and vehicle (F), Torin1 (M), XL388 (N) in NP group. Comparison of activated areas before and after treatment with the vehicle in sham group (G), and vehicle (H), Torin1 (O), XL388 (P) in NP group. A region of interest (ROI) for analyzing the area of activation was expressed using a red circle (a radius of 20 pixels). Data are presented as means ± SEM. *$p < 0.05$, **$p < 0.01$, ***$p < 0.001$ vs. before application of vehicle or mTOR inhibitors, as determined by two-way ANOVA followed by Bonferroni's post-hoc multiple comparison test.

with wide areas of activation, regardless of vehicle application (Fig. 5A). Before Torin1 or XL388 treatment in NP groups, the corresponding groups also showed a similar trend. However, noticeable changes were observed in the IC after Torin1 or XL388 treatment in nerve-injured groups. The duration for which the excitation signals and enlarged areas of activation were observed was diminished after treatment with Torin1 and XL388 in NP groups (Fig. 5B and C).

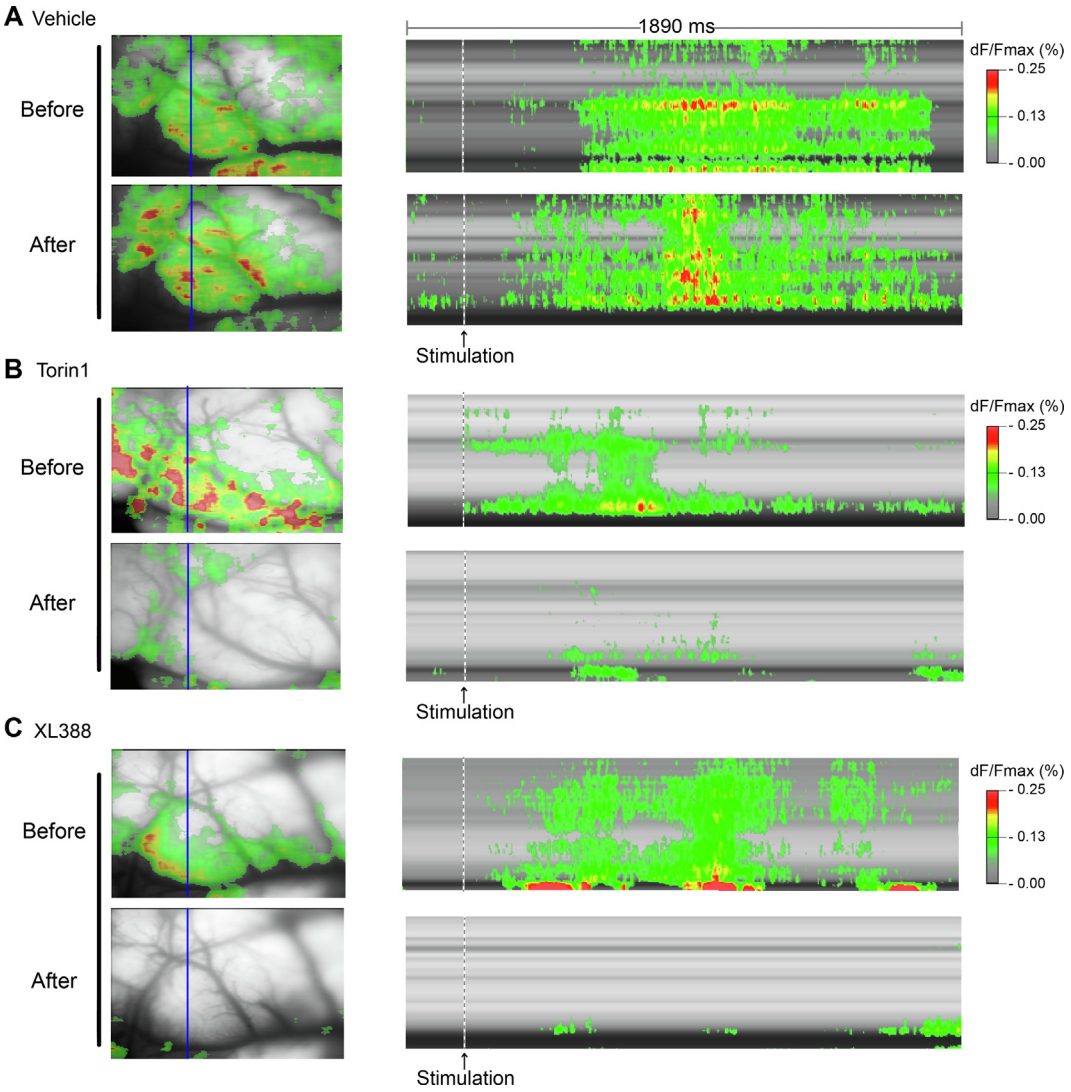

Fig. 5. Representative images of stripe analysis related to optical activity after electrical stimulation of the peripheral receptive field in the injured hind paw before and after vehicle, Torin1, or XL388 treatment. Electrical stimulation of the peripheral receptive field in the injured hind paw was 5 mA in intensity. Stripe images were acquired through optical imaging in vehicle- (A), Torin1- (B), and XL388-treated (C) NP groups. Spatiotemporal activity was acquired from 0 to 1890 ms. Spatiotemporal patterns were obtained from the blue lines on left images. The arrow on the bottom of right picture (dotted lines) shows the time point when electrical stimulation was applied to the injured hind paw.

3. Discussion

The present study showed the efficacy of mTOR inhibitors and recorded the optical signals in the IC after treatment with Torin1 or XL388 under neuropathic condition by using VSD imaging. The mechanical withdrawal threshold was increased by microinjection of mTOR inhibitors as shown by the results of behavioral test. The changes in optical signals of the IC using VSD imaging were observed before and after the application of Torin1 or XL388. Our findings suggested that mTOR inhibitors, Torin1 and XL388, alleviated pain and inhibited optical responses of the IC to peripheral stimulation in the animal model of neuropathy.

3.1. Effect of Torin1 and XL388 on the IC

Neuropathic pain produces spontaneous and abnormal signals in the nervous system. These signals affect the modification of synapses and neurotransmitter properties; therefore, these changes induce synaptic plasticity. In the development of synaptic plasticity, phosphorylated eukaryotic translation initiation factor 4E (eIF4E), eukaryotic translation initiation factor 4E-binding proteins (4EBPs), and ribosomal protein p70 S6 kinase (p70S6K) are mainly involved in the initiation of mRNA translation and protein synthesis (Banko et al., 2005; Klann and Dever, 2004; Pfeiffer and Huber, 2006; Wells, 2006). The mTOR complex has been suggested as an upstream effector that controls these proteins (Klann et al., 2004; Pfeiffer and Huber, 2006). This mTOR complex is known as serine/threonine kinase, and is classified into mTOR complex 1 (mTORC1) and mTOR complex 2 (mTORC2) based on their functions and constituents (Hay and Sonenberg, 2004; Hoeffer and Klann, 2010; Laplante and Sabatini, 2012; Zoncu et al., 2011). The downstream effectors affected by mTORC1 and mTORC2 are different. The downstream effectors of mTORC1 are 4EBP1 and p70S6K (Klann et al., 2004; Pfeiffer and Huber, 2006), and those of mTORC2 are protein kinase B (AKT) and protein kinase C α (PKCα) (Dos et al., 2004; Lee, 2006).

Many studies have reported that the phosphorylation of mTOR complex increased not only in the spinal cord but also in the brain after nerve injury (Lutz et al., 2015; Wang et al., 2015; Zhang et al., 2013). Our previous studies also reported that the changes in phosphorylation of mTOR complex were observed in the IC and ACC after neuropathic

pain developed (Kwon et al., 2017; Um et al., 2018). These studies indicate that mTOR complex is involved in protein synthesis for synaptic plasticity, which leads to mechanical allodynia.

Our previous reports showed that the microinjection of rapamycin into the IC and ACC alleviated the mechanical allodynia following peripheral nerve injury (Kwon et al., 2017; Um et al., 2018). These studies indicated that the alleviation of neuropathic pain is possible through mTOR complex regulation. However, rapamycin is the first-generation mTOR complex inhibitor that has been reported to incompletely inhibit the feedback loop, in addition to showing side effects after long-term use (Guertin and Sabatini, 2009; Lisi et al., 2015). To overcome these limitations, the second-generation mTOR inhibitors were developed. ATP-competitive mTOR inhibitors are among the second-generation mTOR inhibitors; Torin1 and XL388 block both mTORC1 and mTORC2 by targeting the ATP site of the kinase domain of mTOR complex (Albert et al., 2010). ATP-competitive mTOR inhibitors are inhibiting the phosphorylation of downstream effectors of mTORC1 and mTORC2, thereby consequently inhibiting function of mTORC1 and mTORC2 (Albert et al., 2010). Besides, ATP-competitive mTOR inhibitors do not require co-factors such as FK-binding protein 12 (FKBP12) to bind with mTOR complex (Albert et al., 2010; Martelli et al., 2018). These mTOR inhibitors do not cause mutations in the FKBP-rapamycin binding protein (FRB) domain; therefore, they would lead to fewer side effects when taken over a long-term period (Martelli et al., 2018). mTOR complex is included in the phosphatidyl inositol 3′ kinase-related kinases (PIKK) family by its structural similarity (Aylett et al., 2016; Yang and Guan, 2007). There are many kinases in the PIKK family that interact with each other's activities. Especially, phosphoinositide-dependent kinase-1 (PDK1), phosphoinositide 3-kinase (PI3K), and AKT are factors that are known to affect mTOR complex phosphorylation (Obara et al., 2012). Torin1 and XL388 also exert an inhibitory effect over AKT, PDK1, and PI3K, which are included in the PIKK family. Therefore, these features suggest that Torin1 and XL388 are selective and potent inhibitors of mTOR complex.

A previous study related to Torin1 reported evident motor impairment and clinical indications of toxicity in high dose of Torin1 (Obara et al., 2011). The concentration of Torin1 used in the present study did not cause side effects related to motor function, and these results were consistent with a previous study (Cheng et al., 2016). There have been no report on the side effects of XL388 related to sedative or locomotory side effects (Crino, 2016; Martelli et al., 2018). In our experiment, it was necessary to verify the alleviation of neuropathic pain by the second-generation mTOR inhibitors, Torin1 and XL388, that simultaneously block mTORC1 and mTORC2. After microinjection of Torin1 or XL388 into the IC, behavioral test was performed to confirm the efficacy. The most effective time was 4 h after microinjection of Torin1 and XL388. Regarding the mechanical withdrawal threshold, Torin1- and XL388-treated groups showed higher peak values compared to vehicle-treated group. The alleviative effect of Torin1 or XL388 on neuropathic pain did not appear immediately, and this result was similar to that observed in our previous studies, in which the mTOR inhibitor, rapamycin, was microinjected into the IC and ACC under neuropathic condition (Kwon et al., 2017; Um et al., 2018). Therefore, the pain-relieving effect was shown by using ATP-competitive mTOR inhibitors, and these effects are assumed to be due to changes in downstream effectors that were identified in our previous studies (Kwon et al., 2017; Um et al., 2018). These results were short-term effects by single microinjection of Torin1 or XL388 into the IC on POD 7, which would help patients who suffer from neuropathic pain as it will have fewer side effects when taken for a long-term period. Further studies are needed to explore the sedative-related side effects caused by ATP-competitive mTOR inhibitors in clinical cases.

3.2. Changes in neuronal activity after Torin1 and XL388 treatment

Following the behavioral test, identification of the changes in spatiotemporal patterns of optical signals in the IC before and after treatment with Torin1 or XL388 was necessary. Therefore, we performed VSD imaging, which is one of the electrophysiological techniques that records the membrane potential alterations to offer visual validation of the activity of neuronal population (An et al., 2012). Our previous study demonstrated that neuropathic rats showed more sensitive optical responses to the electrical stimulation of peripheral receptive field than sham-injured rats did (Han et al., 2016). Besides, neuropathic rats also showed highly activated signals in the IC and ACC under neuropathic condition before rapamycin treatment (Kwon et al., 2017; Um et al., 2018). Similarly, we observed that the peak amplitudes increased and the activated areas widened with an increase in the intensity of electrical stimulation of the hind paw before treatment with the vehicle, Torin1, or XL388 in neuropathic rats. The peak amplitudes of optical signals and activated areas were highly correlated with the intensity of peripheral stimulation before treatment; however, the correlation became lowered after treatment of Torin1 or XL388. Also, it was shown that the peak amplitude of optical signals at 0 mA of electrical intensity was not completely 0, regardless of the application of before and after Torin1 or XL388. The reason for the noise of optical signals is related to the respiration and heart rate of experimental animals; besides, the noise of optical signals could be due to the noise from connecting wires or the device itself in the external environment.

The inhibition of mTORC1 and mTORC2 is expected to alleviate excessive neuronal activity in the IC resulting from neuropathic pain induced by nerve injury. Additionally, we observed distinctive changes in optical signals under neuropathic condition after Torin1 or XL388 treatment of the IC. In vehicle-treated group, there were no significant changes in peak amplitudes and excitatory areas of cortical activity. Unlike vehicle-treated group, Torin1- and XL388-treated groups showed a decrease in the peak amplitudes and excitatory areas of cortical activity in the IC after treatment. The decreased activation of the IC indicates that nerve-injured rats perceived less pain after Torin1 or XL388 treatment. These results show that inhibition of both mTORC1 and mTORC2 alleviates neuropathic pain.

The roles of mTORC1 and mTORC2 in synaptic plasticity are different. It is known that mTORC1 is involved in mRNA translation and mTORC2 is involved in cytoskeletal rearrangement, which generates structure or junction of synapses (Kelleher et al., 2004; Oh and Jacinto, 2011; Pfeiffer and Huber, 2006). Differences in their roles are due to the differences in downstream effectors of mTORC1 and mTORC2 (Dos et al., 2004; Lee, 2006). Torin1 and XL388 are ATP-competitive mTOR inhibitors, which simultaneously inhibit the phosphorylation of both mTORC1 and mTORC2 (Guertin and Sabatini, 2009; Liu et al., 2010; Takeuchi et al., 2013). Since our previous studies confirmed the changes induced in downstream effectors of mTORC1 by rapamycin (Kwon et al., 2017; Um et al., 2018), we suggest that the downstream effectors of mTORC1 and mTORC2 leading to the development of synaptic plasticity might be altered by Torin1 and XL388. Therefore, the changed expression levels of downstream phosphorylated effectors affected mRNA translation and cytoskeletal rearrangement for generating synaptic plasticity. These results indicate that a pain-relieving effect is shown when mRNA translation and cytoskeletal rearrangement are suppressed together. Our study suggests that the inhibition of mTORC1 and mTORC2 effectively contribute to the improved alleviation of neuropathic pain.

3.3. Visible evidence of neural plasticity on optical imaging

In this study, we spatiotemporally mapped the neuronal activity of the IC. Our findings indicated that the activated areas were enlarged, and that the signals lasted longer in neuropathic rats. Additionally, the decline in neural activity was observed as a result of mTOR inhibition. These findings showed that mTOR inhibition has a pain-relieving effect on severe neuropathic symptoms, and that it alleviates the hyper-activated neuronal activities in the IC. Previous studies showed that the

optical signals of the IC increased depending on the intensity of electrical stimulation of peripheral receptive field in neuropathic rats (Cha et al., 2009; Han et al., 2016). These studies indicated that enlarged activated areas and long-lasting neural activities in the IC after electrical stimulation could explain the increased depolarization of neurons in the cortex of nerve-injured rats. Based on these studies, we assumed that neuronal excitation in neuropathy could be explained by the mTOR pathway, and needed to further explore molecular changes by inhibition of both mTORC1 and mTORC2 in neuropathic pain condition.

Although optical imaging detects direct changes in cortical activity, it can only observe cortical signals in a limited window. Due to this limitation, we could not analyze the interactions of other pain-related areas with the IC, as well as the responses between deep brain regions and the IC. Nociceptive signals from the peripheral nerve injury have been known to be transmitted to the thalamus through spinothalamic tract, and these signals can activate the thalamus and other regions, such as the prefrontal cortex, S1, S2, motor cortex, and ACC (Gogolla, 2017; Jaggi and Singh, 2011; Zhuo, 2008). Although nociceptive signals from the peripheral nerves can be directly transported to the IC, there were also indirect pathways that convey nociceptive signals to the IC through other pain-related brain regions (Gogolla, 2017). Therefore, the temporal kinetics of responses such as latency, duration, and time to peak in the IC would be diversified. Further studies are needed to explore the pathways between the IC and cortical or subcortical areas.

In conclusion, we observed the alleviative effect of ATP-competitive mTOR inhibitors on neuropathic pain. Mechanical allodynia induced by nerve injury was relieved in neuropathic rats after microinjection of Torin1 or XL388 into the IC. Optical imaging using VSD showed that the peak amplitudes of optical signals and the size of activated areas in the IC were reduced after treatments with Torin1 or XL388. Pain-relieving effect was the result of inhibition of both mTORC1 and mTORC2. Nevertheless, it is difficult to determine whether mTORC1 or mTORC2 has a greater effect on the neuropathic pain mechanism.

4. Experimental procedures

4.1. Experimental animals

Male Sprague-Dawley rats (weight, 250–280 g; Harlan, Koatec, Pyeongtaek, Korea) were used for this study. All procedures adhered to the National Institutes of Health guidelines, and were approved by the Institutional Animal Care and Use Committee of Yonsei University Health System (permit no. 2017–0076). Rats were allowed to acclimate for 7 days after arrival; three animals were housed per cage and exposed to 12-h light/dark cycles. Food and water were provided ad libitum. The number of rats used in the experiment were 11 in sham group and 16 per vehicle, Torin1, and XL388 groups, respectively.

4.2. Neuropathic surgery and cannula implantation

Nerve injury was induced as previously described (Lee et al., 2000), following the period of acclimation. Rats were placed in the induction chamber for anesthesia. A mixture of 5% vaporized isoflurane and oxygen (2 L/min) was supplied into the induction chamber, and rats were pulled out when their whiskers became motionless. An anesthetic mask was placed on the snouts of rats to supply the same anesthetic gas during surgery. The left sciatic nerve and its branches were exposed by making an incision in the skin and muscles right above them. Tibial and sural nerves were tightly ligated using 5–0 black silk and sectioned, whereas common peroneal nerve was left intact. All surgical procedures were performed within 20 min per rat, and the rats in sham-injured group were subjected to an identical surgery without nerve injury. Under sodium pentobarbital (50 mg/kg, intraperitoneal injection [i.p.]) anesthesia, rats were placed into stereotaxic frame. Guide cannula was positioned according to the location, and bilaterally implanted into the rostral anterior IC (1.0 mm anterior to bregma, ± 4.7 mm lateral from the midline, 5.8 mm below the surface of the skull (Han et al., 2015; Jung et al., 2016; Kwon et al., 2017; Wu et al., 2016)). Rats were allowed to recover for 1 week after cannula implantation.

4.3. Mechanical allodynia test

Mechanical allodynia test was performed 1 day before neuropathic surgery and on POD 1, 4, and 7. On POD 7, each rat was placed in a squared acrylic cage with a metal mesh floor, and was allowed to habituate for 15 min. The test was performed using an electrical von Frey filament (no. 38450; UGO Basile, Varese, Italy). Filament was placed vertically on the skin surface of the medial side of left hind paw, and force values were measured until the animal exhibited withdrawal or licked the hind paw. The measurements were repeated seven times with 2- to 3-minute intervals. The collected data, excluding the maximum and minimum values, were averaged. All tests were performed in a double-blinded fashion. Behavioral test was conducted before and 0.5, 1, 2, 4, 8, 12, 24 h after microinjection of Torin1 (No. 4247, Tocris, Bristol, England), XL388 (No. 4893, Tocris), or vehicle on POD 7. Behavioral test was performed on POD 7 to inhibit the synaptic plasticity that might induce mechanical allodynia due to synaptic plasticity in the IC by directly infused Torin1 or XL388.

4.4. Microinjection of Torin1 and XL388 into the IC

In this study, we used two types of second-generation mTOR complex inhibitors: Torin1 and XL388. These inhibitors were diluted in 0.06% DMSO in saline. Saline-based 0.06% DMSO was used as vehicle. Behavioral tests to determine the dose-dependent effects of Torin1 and XL388 were conducted to apply the appropriate concentration in the IC (Supplementary Fig. 3 and Fig. 4). The most effective concentration was 400 nM for Torin1, and 500 nM for XL388. On POD 7, 0.5 μl of Torin1 (400 nM), XL388 (500 nM), or vehicle was directly infused into the IC bilaterally using the injection cannula with Hamilton syringes and PE-10 tubing. The inhibitor or vehicle was injected at the rate of 0.5 μl/min, and subsequently, injection cannula was placed in position for an additional 1 min to prevent reflux along the injection cannula.

4.5. Optical imaging of the IC

The rats were re-anesthetized using urethane (1.25 g/kg, i.p.) on POD 7. Urethane is the appropriate anesthetic drug for optical imaging, since deep and long anesthesia does not interfere with neural function. Infusion of the appropriate amount of urethane does not significantly affect neural activity (Devonshire et al., 2010). To prevent mucus secretion, which is a side effect of urethane, atropine (5 mg/kg, i.p.) was administered to rats. Dexamethasone sulfate (1 mg/kg, i.p.) was also administered to prevent the brain from swelling. Heart rate was monitored by electrocardiography, and body temperature was maintained at 36 ˚C using a rectal probe and heating pad system (Homeothermic Blanket Control Unit, Harvard Apparatus, Holliston, MA, USA). After all of the injections were administered, we waited until the rats were anesthetized. Then, rats were placed on the custom-made stereotaxic frame. To ensure easy access to the IC, which is anterolaterally located in the brain, rats were placed in a lateral position (Supplementary Fig. 5). To induce local anesthesia, lidocaine was injected into the skin and muscle of rats. After incising the skin, the muscular layer—which covers the skull—was removed, and the zygomatic arch was revealed. It was necessary to remove the zygomatic arch using a bone cutter to pull the 4–0 black silk over the jaw-bone. If bleeding was severe, hemostatic compound (ViscoStat®, Ultradent Products, Inc, South Jordan, UT, USA) was used to stop the bleeding. Craniectomy was performed with extreme care, since the internal maxillary vein is located beside the zygomatic arch and superficial temporal vein. After craniectomy, dura mater was also removed carefully to avoid injuring the cortex. To prevent drying and bleeding, saline-soaked cotton balls were placed on

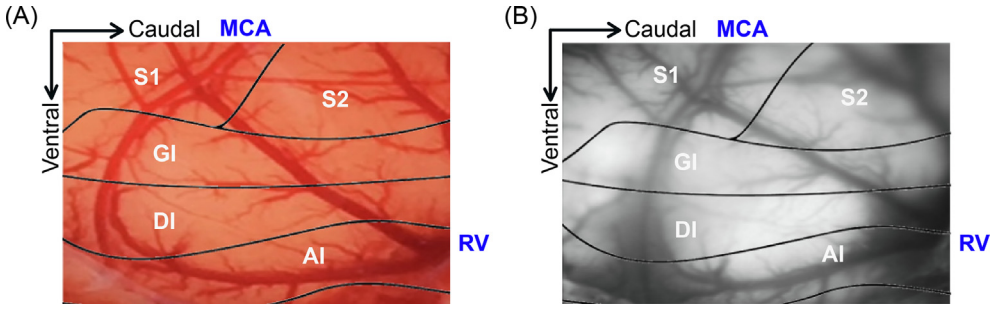

Fig. 6. Image acquisition using optical imaging system. (A) Lateral view of the IC before optical imaging. (B) Reconstruction image viewed through an optical imaging system. Black lines in (A) and (B) indicate boundaries of regions in the brain.

the cortex. Finally, the exposed region of the IC was stained using a VSD (di-2-ANEPEQ, 50 μg/mL in saline, Molecular Proves, Eugene, OR, USA) for 1 h and subsequently, rinsed with saline observantly (Fig. 6A). The surface of the brain was captured via digital camera, and the captured image was edited to match the optical images to provide image of the actual imaging site (Fig. 6A). For electrical stimulation of peripheral receptive field, a pair of stainless-steel electrodes was penetrated into the injured hind paws where the electronic von Frey filament was placed during behavioral test. Stimulation was applied in the form of square pulse (width: 0.1 ms, interstimulus interval: 5 s, intensity: 0, 0.6, 1.25, 2.5, and 5.0 mA) using a stimulus isolation unit (World Precision Instruments, Sarasota, FL, USA).

Optical imaging was performed as previously described (Cha et al., 2009; Han et al., 2016). An optical microscope (Leica Microsystems Ltd., Heerbrugg, Switzerland), equipped with a 1× objective and 1× projection lens, was positioned on the upper side of recording site. Neuronal signals were detected using an optical imaging system consisting of a high-resolution CCD camera (Brainvision Inc., Tokyo, Japan) equipped with a dichroic mirror with 510–550 nm excitation filter and 590 nm absorption filter. A tungsten halogen lamp (150 W) was used as the source of fluorescence. The imaging area was approximately 6.4 × 4.8 mm^2, and consisted of 184 × 124 pixels (Fig. 6B). Detailed explanations of optical imaging are provided in Supplementary Fig. 5. Optical images were acquired before and after the application of vehicle, Torin1, or XL388 directly to the exposed the IC for 30 min. The concentration of 0.06% DMSO in saline for vehicle, 400 nM of Torin1, or 500 nM of XL388 was applied on cortical surface in optical imaging. These were the same concentrations as those used in the behavioral test. After optical imaging, rats were euthanized by an overdose of urethane.

4.6. VSD imaging analysis

The change in fluorescence intensity was observed for 1890 ms during each trial. Optical signals were acquired using an optical imaging recording system (MICAM02, Brainvision Inc.) at a rate of 3.7 ms/frame and averaged 20 times. Optical image acquisition was triggered by electrocardiogram signals using a stimulus/non-stimulus subtraction method. The ratio of intensity of fluorescence (ΔF) in each pixel relative to the initial fluorescence intensity (F) was revealed as a fractional change (ΔF/F) to normalize the value of each pixel. Amplitudes and excited areas of optical signals were calculated using a spatial filter (9 × 9 pixels). The artifacts resulting from vibration and brain movements were removed using a spatial filter. Data were collected and identified using BV Analyzer software (Brainvision Inc.). The fractional changes in optical signals (i.e., optical intensity) and areas of activation were quantified. Changes in optical intensity in the IC were identified as a percentage of fractional change in fluorescence (%ΔF/F). Activated areas were described as the number of activated pixels divided by the total number of pixels, which was expressed as a percentage of ROI. ROI was set at a radius of 20 pixels to analyze the activation area of optical signals. All data on optical intensity and activated areas were analyzed using BV Analyzer software (Brainvision Inc.).

4.7. Statistical analysis

Statistical analyses were performed using GraphPad Prism (Graphpad Software, San Diego, CA, USA). All values are presented as mean ± SEM. Differences in mechanical withdrawal thresholds observed during the behavioral test were analyzed using two-way ANOVA, followed by Bonferroni's post-hoc multiple comparison test. Pearson's correlation coefficient was used to determine the correlation between peak amplitudes of optical signals and intensity of electrical stimulation in peripheral receptive field. The correlation coefficient was compared to 0 by one sample *t*-test. Differences in intensities of optical signals and areas of activation were analyzed using paired *t*-test. P values less than 0.05 were considered statistically significant.

Declaration of interests

None.

CRediT authorship contribution statement

Kyeongmin Kim: Conceptualization, Formal analysis, Investigation, Data curation, Visualization, Writing - original draft, Writing - review & editing. **Songyeon Choi:** Conceptualization, Formal analysis, Data curation, Writing - original draft, Writing - review & editing. **Myeounghoon Cha:** Conceptualization, Methodology, Writing - original draft, Writing - review & editing. **Bae Hwan Lee:** Conceptualization, Funding acquisition, Project administration, Resources, Supervision, Writing - original draft, Writing - review & editing.

Acknowledgement

The authors would like to thank MID (Medical Illustration & Design), a part of the Medical Research Support Services of Yonsei University College of Medicine, for all of the artistic support related to this work. Funding sources: This work was supported by the National Research Foundation of Korea (NRF) grant funded by the Korean government (MSIT) (2017R1A2B3005753). Conflicts of interest disclosure: There are no conflicts of interest arising from the research reported in this article.

Appendix A. Supplementary data

Supplementary data to this article can be found online at https://doi.org/10.1016/j.brainres.2020.146720.

References

Albert, S., Serova, M., Dreyer, C., Sablin, M.P., Faivre, S., Raymond, E., 2010. New inhibitors of the mammalian target of rapamycin signaling pathway for cancer. Expert Opin. Invest. Drugs 19, 919–930. https://doi.org/10.1517/13543784.2010.499121.

An, S., Yang, J.W., Sun, H., Kilb, W., Luhmann, H.J., 2012. Long-term potentiation in the neonatal rat barrel cortex in vivo. J. Neurosci. 32, 9511–9516. https://doi.org/10.1523/jneurosci.1212-12.2012.

Apkarian, A.V., Bushnell, M.C., Treede, R.-D., Zubieta, J.-K., 2005. Human brain mechanisms of pain perception and regulation in health and disease. Eur. J. Pain 9, 463–484. https://doi.org/10.1016/j.ejpain.2004.11.001.

Aylett, C.H.S., Sauer, E., Imseng, S., Boehringer, D., Hall, M.N., Ban, N., Maier, T., 2016. Architecture of human mTOR complex 1. Science 351, 48. https://doi.org/10.1126/science.aaa3870.

Banko, J.L., Poulin, F., Hou, L., DeMaria, C.T., Sonenberg, N., Klann, E., 2005. The translation repressor 4E-BP2 is critical for eIF4F complex formation, synaptic plasticity, and memory in the hippocampus. J. Neurosci. 25, 9581–9590. https://doi.org/10.1523/jneurosci.2423-05.2005.

Basbaum, A.I., Bautista, D.M., Scherrer, G., Julius, D., 2009. Cellular and molecular mechanisms of pain. Cell 139, 267–284. https://doi.org/10.1016/j.cell.2009.09.028.

Baumgärtner, U., Iannetti, G.D., Zambreanu, L., Stoeter, P., Treede, R.-D., Tracey, I., 2010. Multiple somatotopic representations of heat and mechanical pain in the operculo-insular cortex: A high-resolution fMRI study. J. Neurophysiol. 104, 2863–2872. https://doi.org/10.1152/jn.00253.2010.

Callin, S., Bennett, M.I., 2008. Assessment of neuropathic pain. BJA Educ. 8, 210–213. https://doi.org/10.1093/bjaceaccp/mkn037.

Cha, M., Um, S.W., Kwon, M., Nam, T.S., Lee, B.H., 2017. Repetitive motor cortex stimulation reinforces the pain modulation circuits of peripheral neuropathic pain. Sci. Rep. 7, 7986. https://doi.org/10.1038/s41598-017-08208-2.

Cha, M.H., Kim, D.S., Cho, Z.H., Sohn, J.H., Chung, M.A., Lee, H.J., Nam, T.S., Lee, B.H., 2009. Modification of cortical excitability in neuropathic rats: a voltage-sensitive dye study. Neurosci. Lett. 464, 117–121. https://doi.org/10.1016/j.neulet.2009.08.024.

Chae, Y., Park, H.J., Hahm, D.H., Lee, B.H., Park, H.K., Lee, H., 2010. Spatiotemporal patterns of neural activity in response to electroacupuncture stimulation in the rodent primary somatosensory cortex. Neurol. Res. 32 (Suppl. 1), 64–68. https://doi.org/10.1179/016164109x12537002794084.

Cheng, N.T., Guo, A., Cui, Y.P., 2016. Intra-articular injection of Torin 1 reduces degeneration of articular cartilage in a rabbit osteoarthritis model. Bone Joint Res. 5, 218–224. https://doi.org/10.1302/2046-3758.56.Bjr-2015-0001.

Coffeen, U., Manuel Ortega-Legaspi, J., Lopez-Munoz, F.J., Simon-Arceo, K., Jaimes, O., Pellicer, F., 2011. Insular cortex lesion diminishes neuropathic and inflammatory pain-like behaviours. Eur. J. Pain 15, 132–138. https://doi.org/10.1016/j.ejpain.2010.06.007.

Craig, A.D., Chen, K., Bandy, D., Reiman, E.M., 2000. Thermosensory activation of insular cortex. Nat. Neurosci. 3, 184. https://doi.org/10.1038/72131.

Crino, P.B., 2016. The mTOR signalling cascade: paving new roads to cure neurological disease. Nat. Rev. Neurol. 12, 379. https://doi.org/10.1038/nrneurol.2016.81.

Devonshire, I.M., Grandy, T.H., Dommett, E.J., Greenfield, S.A., 2010. Effects of urethane anaesthesia on sensory processing in the rat barrel cortex revealed by combined optical imaging and electrophysiology. Eur. J. Neurosci. 32, 786–797. https://doi.org/10.1111/j.1460-9568.2010.07322.x.

Dos, D.S., Ali, S.M., Kim, D.-H., Guertin, D.A., Latek, R.R., Erdjument-Bromage, H., Tempst, P., Sabatini, D.M., 2004. Rictor, a novel binding partner of mTOR, defines a rapamycin-insensitive and raptor-independent pathway that regulates the cytoskeleton. Curr. Biol. 14, 1296–1302. https://doi.org/10.1016/j.cub.2004.06.054.

Fehervari, T.D., Okazaki, Y., Sawai, H., Yagi, T., 2015. In vivo voltage-sensitive dye study of lateral spreading of cortical activity in mouse primary visual cortex induced by a current impulse. PLoS One 10, e0133853. https://doi.org/10.1371/journal.pone.0133853.

Ferezou, I., Matyas, F., Petersen, C.C.H., 2009. Imaging the brain in action: real-time voltage-sensitive dye imaging of sensorimotor cortex of awake behaving mice. In: Frostig, R.D. (Ed.), In Vivo Optical Imaging Of Brain Function, second ed. CRC Press, Boca Raton, pp. 177–188.

Fujita, S., Adachi, K., Koshikawa, N., Kobayashi, M., 2010. Spatiotemporal dynamics of excitation in rat insular cortex: intrinsic corticocortical circuit regulates caudal-rostro excitatory propagation from the insular to frontal cortex. Neuroscience 165, 278–292. https://doi.org/10.1016/j.neuroscience.2009.09.073.

Garcia-Larrea, L., Peyron, R., 2013. Pain matrices and neuropathic pain matrices: a review. Pain 154 (Suppl. 1), S29–S43. https://doi.org/10.1016/j.pain.2013.09.001.

Gogolla, N., 2017. The insular cortex. Curr. Biol. 27, R580–R586. https://doi.org/10.1016/j.cub.2017.05.010.

Guertin, D.A., Sabatini, D.M., 2009. The pharmacology of mTOR inhibition. Sci. Signal. 2, pe24. https://doi.org/10.1126/scisignal.267pe24.

Han, J., Cha, M., Kwon, M., Hong, S.-K., Bai, S.J., Lee, B.H., 2016. In vivo voltage-sensitive dye imaging of the insular cortex in nerve-injured rats. Neurosci. Lett. 634, 146–152. https://doi.org/10.1016/j.neulet.2016.10.015.

Han, J., Kwon, M., Cha, M., Tanioka, M., Hong, S.K., Bai, S.J., Lee, B.H., 2015. Plasticity-related PKMzeta signaling in the insular cortex is involved in the modulation of neuropathic pain after nerve injury. Neural Plast. 2015, 601767. https://doi.org/10.1155/2015/601767.

Hay, N., Sonenberg, N., 2004. Upstream and downstream of mTOR. Genes Dev. 18, 1926–1945. https://doi.org/10.1101/gad.1212704.

Hess, A., Sergejeva, M., Budinsky, L., Zeilhofer, H.U., Brune, K., 2007. Imaging of hyperalgesia in rats by functional MRI. Eur. J. Pain 11, 109–119. https://doi.org/10.1016/j.ejpain.2006.01.005.

Hoeffer, C.A., Klann, E., 2010. mTOR signaling: at the crossroads of plasticity, memory and disease. Trends Neurosci. 33, 67–75. https://doi.org/10.1016/j.tins.2009.11.003.

Jaggi, A.S., Singh, N., 2011. Role of different brain areas in peripheral nerve injury-induced neuropathic pain. Brain Res. 1381, 187–201. https://doi.org/10.1016/j.brainres.2011.01.002.

Jasmin, L., Burkey, A.R., Granato, A., Ohara, P.T., 2004. Rostral agranular insular cortex and pain areas of the central nervous system: a tract-tracing study in the rat. J. Comp. Neurol. 468, 425–440. https://doi.org/10.1002/cne.10978.

Jung, H.H., Shin, J., Kim, J., Ahn, S.H., Lee, S.E., Koh, C.S., Cho, J.S., Kong, C., Shin, H.C., Kim, S.J., Chang, J.W., 2016. Rostral agranular insular cortex lesion with motor cortex stimulation enhances pain modulation effect on neuropathic pain model. Neural Plast. 2016, 3898924. https://doi.org/10.1155/2016/3898924.

Kelleher 3rd, R.J., Govindarajan, A., Tonegawa, S., 2004. Translational regulatory mechanisms in persistent forms of synaptic plasticity. Neuron 44, 59–73. https://doi.org/10.1016/j.neuron.2004.09.013.

Kim, M.J., Tanioka, M., Um, S.W., Hong, S.K., Lee, B.H., 2018. Analgesic effects of FAAH inhibitor in the insular cortex of nerve-injured rats. Mol. Pain 14. https://doi.org/10.1177/1744806918814345.

Klann, E., Antion, M.D., Banko, J.L., Hou, L., 2004. Synaptic plasticity and translation initiation. Learn. Mem. 11, 365–372. https://doi.org/10.1101/lm.79004.

Klann, E., Dever, T.E., 2004. Biochemical mechanisms for translational regulation in synaptic plasticity. Nat. Rev. Neurosci. 5, 931–942. https://doi.org/10.1038/nrn1557.

Kobayashi, M., Fujita, S., Takei, H., Song, L., Chen, S., Suzuki, I., Yoshida, A., Iwata, K., Koshikawa, N., 2010. Functional mapping of gustatory neurons in the insular cortex revealed by pERK-immunohistochemistry and in vivo optical imaging. Synapse 64, 323–334. https://doi.org/10.1002/syn.20731.

Kuner, R., 2010. Central mechanisms of pathological pain. Nat. Med. 16, 1258. https://doi.org/10.1038/nm.2231.

Kuner, R., Flor, H., 2016. Structural plasticity and reorganisation in chronic pain. Nat. Rev. Neurosci. 18, 20–30. https://doi.org/10.1038/nrn.2016.162.

Kwon, M., Han, J., Kim, U.J., Cha, M., Um, S.W., Bai, S.J., Hong, S.K., Lee, B.H., 2017. Inhibition of Mammalian Target of Rapamycin (mTOR) Signaling in the Insular Cortex Alleviates Neuropathic Pain after Peripheral Nerve Injury. Front. Mol. Neurosci. 10, 79. https://doi.org/10.3389/fnmol.2017.00079.

Laplante, M., Sabatini, D.M., 2012. mTOR signaling in growth control and disease. Cell 149, 274–293. https://doi.org/10.1016/j.cell.2012.03.017.

Lee, B.H., Won, R., Baik, E.J., Lee, S.H., Moon, C.H., 2000. An animal model of neuropathic pain employing injury to the sciatic nerve branches. NeuroReport 11, 657–661. https://doi.org/10.1097/00001756-200003200-00002.

Lee, H.K., 2006. Synaptic plasticity and phosphorylation. Pharmacol. Ther. 112, 810–832. https://doi.org/10.1016/j.pharmthera.2006.06.003.

Li, X.-Y., Ko, H.-G., Chen, T., Descalzi, G., Koga, K., Wang, H., Kim, S.S., Shang, Y., Kwak, C., Park, S.-W., Shim, J., Lee, K., Collingridge, G.L., Kaang, B.-K., Zhuo, M., 2010. Alleviating neuropathic pain hypersensitivity by inhibiting PKMζ in the anterior cingulate cortex. Science 330, 1400. https://doi.org/10.1126/science.1191792.

Li, X.Y., Wan, Y., Tang, S.J., Guan, Y., Wei, F., Ma, D., 2016. Maladaptive plasticity and neuropathic pain. Neural Plast. 2016, 4842159. https://doi.org/10.1155/2016/4842159.

Lisi, L., Aceto, P., Navarra, P., Dello Russo, C., 2015. mTOR kinase: a possible pharmacological target in the management of chronic pain. Biomed Res. Int. 2015, 394257. https://doi.org/10.1155/2015/394257.

Liu, Q., Chang, J.W., Wang, J., Kang, S.A., Thoreen, C.C., Markhard, A., Hur, W., Zhang, J., Sim, T., Sabatini, D.M., Gray, N.S., 2010. Discovery of 1-(4-(4-propionylpiperazin-1-yl)-3-(trifluoromethyl)phenyl)-9-(quinolin-3-yl)benz o[h][1,6]naphthyridin-2(1H)-one as a highly potent, selective mammalian target of rapamycin (mTOR) inhibitor for the treatment of cancer. J. Med. Chem. 53, 7146–7155. https://doi.org/10.1021/jm101144f.

Liu, Q., Thoreen, C., Wang, J., Sabatini, D., Gray, N.S., 2009. mTOR mediated anti-cancer drug discovery. Drug Discov. Today Ther. Strateg. 6, 47–55. https://doi.org/10.1016/j.ddstr.2009.12.001.

Lorenz, J., Casey, K.L., 2005. Imaging of acute versus pathological pain in humans. Eur. J. Pain 9, 163–165. https://doi.org/10.1016/j.ejpain.2004.07.009.

Lorenz, J., Cross, D.J., Minoshima, S., Morrow, T.J., Paulson, P.E., Casey, K.L., 2002. A unique representation of heat allodynia in the human brain. Neuron 35, 383–393. https://doi.org/10.1016/s0896-6273(02)00767-5.

Lu, C., Yang, T., Zhao, H., Zhang, M., Meng, F., Fu, H., Xie, Y., Xu, H., 2016. Insular cortex is critical for the perception, modulation, and chronification of pain. Neurosci. Bull. 32, 191–201. https://doi.org/10.1007/s12264-016-0016-y.

Luo, C., Kuner, T., Kuner, R., 2014. Synaptic plasticity in pathological pain. Trends Neurosci. 37, 343–355. https://doi.org/10.1016/j.tins.2014.04.002.

Lutz, A., McFarlin, D.R., Perlman, D.M., Salomons, T.V., Davidson, R.J., 2013. Altered anterior insula activation during anticipation and experience of painful stimuli in expert meditators. Neuroimage 64, 538–546. https://doi.org/10.1016/j.neuroimage.2012.09.030.

Lutz, B.M., Nia, S., Xiong, M., Tao, Y.-X., Bekker, A., 2015. mTOR, a new potential target for chronic pain and opioid-induced tolerance and hyperalgesia. s12990–12015-10030-12995. Mol. Pain 11. https://doi.org/10.1186/s12990-015-0030-5.

Martelli, A.M., Buontempo, F., McCubrey, J.A., 2018. Drug discovery targeting the mTOR pathway. Clin. Sci. (Lond) 132, 543–568. https://doi.org/10.1042/cs20171158.

Metz, A.E., Yau, H.-J., Centeno, M.V., Apkarian, A.V., Martina, M., 2009. Morphological and functional reorganization of rat medial prefrontal cortex in neuropathic pain. Proc. Natl. Acad. Sci. 106, 2423. https://doi.org/10.1073/pnas.0809897106.

Obara, I., Geranton, S.M., Hunt, S.P., 2012. Axonal protein synthesis: a potential target for pain relief? Curr. Opin. Pharmacol. 12, 42–48. https://doi.org/10.1016/j.coph.2011.

10.005.
Obara, I., Tochiki, K.K., Geranton, S.M., Carr, F.B., Lumb, B.M., Liu, Q., Hunt, S.P., 2011. Systemic inhibition of the mammalian target of rapamycin (mTOR) pathway reduces neuropathic pain in mice. Pain 152, 2582–2595. https://doi.org/10.1016/j.pain.2011.07.025.
Oh, W.J., Jacinto, E., 2011. mTOR complex 2 signaling and functions. Cell Cycle 10, 2305–2316. https://doi.org/10.4161/cc.10.14.16586.
Paxinos, G., Watson, C., 2006. The Rat Brain in Stereotaxic Coordinates: Hard, Cover Edition. Elsevier Science.
Pfeiffer, B.E., Huber, K.M., 2006. Current advances in local protein synthesis and synaptic plasticity. J. Neurosci. 26, 7147. https://doi.org/10.1523/JNEUROSCI.1797-06.2006.
Takeuchi, C.S., Kim, B.G., Blazey, C.M., Ma, S., Johnson, H.W., Anand, N.K., Arcalas, A., Baik, T.G., Buhr, C.A., Cannoy, J., Epshteyn, S., Joshi, A., Lara, K., Lee, M.S., Wang, L., Leahy, J.W., Nuss, J.M., Aay, N., Aoyama, R., Foster, P., Lee, J., Lehoux, I., Munagala, N., Plonowski, A., Rajan, S., Woolfrey, J., Yamaguchi, K., Lamb, P., Miller, N., 2013. Discovery of a novel class of highly potent, selective, ATP-competitive, and orally bioavailable inhibitors of the mammalian target of rapamycin (mTOR). J. Med. Chem. 56, 2218–2234. https://doi.org/10.1021/jm3007933.
Um, S.W., Kim, M.J., Leem, J.W., Bai, S.J., Lee, B.H.J.M.N., 2018. Pain-relieving effects of mTOR inhibitor in the anterior cingulate cortex of neuropathic rats. Mol. Neurobiol. https://doi.org/10.1007/s12035-018-1245-z.
Vilar, E., Perez-Garcia, J., Tabernero, J., 2011. Pushing the envelope in the mTOR pathway: the second generation of inhibitors. Mol. Cancer Ther. 10, 395–403. https://doi.org/10.1158/1535-7163.Mct-10-0905.
Wang, J., Feng, D.Y., Li, Z.H., Feng, B., Zhang, H., Zhang, T., Chen, T., Li, Y.Q., 2015. Activation of the mammalian target of rapamycin in the rostral ventromedial medulla contributes to the maintenance of nerve injury-induced neuropathic pain in rat. Neural Plast. 2015, 394820. https://doi.org/10.1155/2015/394820.
Wells, D.G., 2006. RNA-binding proteins: a lesson in repression. J. Neurosci. 26, 7135–7138. https://doi.org/10.1523/jneurosci.1795-06.2006.
Wu, W.Y., Liu, C.Y., Tsai, M.L., Yen, C.T., 2016. Nocifensive behavior-related laser heat-evoked component in the rostral agranular insular cortex revealed using morphine analgesia. Physiol. Behav. 154, 129–134. https://doi.org/10.1016/j.physbeh.2015.11.020.
Xu, B., Descalzi, G., Ye, H.R., Zhuo, M., Wang, Y.W., 2012. Translational investigation and treatment of neuropathic pain. Mol. Pain 8, 15. https://doi.org/10.1186/1744-8069-8-15.
Yang, Q., Guan, K.-L., 2007. Expanding mTOR signaling. Cell Res. 17, 666–681. https://doi.org/10.1038/cr.2007.64.
Zhang, W., Sun, X.-F., Bo, J.-H., Zhang, J., Liu, X.-J., Wu, L.-P., Ma, Z.-L., Gu, X.-P., 2013. Activation of mTOR in the spinal cord is required for pain hypersensitivity induced by chronic constriction injury in mice. Pharmacol. Biochem. Behav. 111, 64–70. https://doi.org/10.1016/j.pbb.2013.07.017.
Zhuo, M., 2008. Cortical excitation and chronic pain. Trends Neurosci. 31, 199–207. https://doi.org/10.1016/j.tins.2008.01.003.
Zoncu, R., Efeyan, A., Sabatini, D.M., 2011. mTOR: from growth signal integration to cancer, diabetes and ageing. Nat. Rev. Mol. Cell Biol. 12, 21–35. https://doi.org/10.1038/nrm3025.